Relationship between Retinal Nerve Fiber Layer and Visual Field Sensitivity as Measured by Optical Coherence Tomography in Chiasmal Compression

Helen V. Danesh-Meyer,[1] *Stuart C. Carroll,*[1] *Rod Foroozan,*[2] *Peter J. Savino,*[3] *Jennifer Fan,*[1] *Yannan Jiang,*[4] *and Stephen Vander Hoorn*[4]

Purpose. To investigate the spatial relationship between retinal nerve fiber layer (RNFL) thickness measured with optical coherence tomography (OCT) and visual field sensitivity (VFS) measured by standard automated perimetry (SAP) in chiasmal compression.

Methods. Twenty-six patients with chiasmal compression were enrolled. RNFL thickness was measured with the StratusOCT and VFS with SAP (Humphrey Field Analyzer; both from Carl Zeiss Meditec, Dublin, CA). Relationships between RNFL thickness (in clock hours, hemifields, and sectors) and VFS (zones were divided into hemifields, quadrants, and sectors based on a validated visual field map) expressed in a decibel scale and 1/lambert (L) were evaluated by linear and nonlinear regression. Coefficients of determination (R^2) were calculated by using a multivariate model.

Results. Average RNFL thickness correlated strongly with pattern standard deviation (PSD; $R = 0.622$) and mean deviation (MD; $R = 0.413$). The four strongest correlations were between the 8 o'clock OCT position (temporal disc), with the temporal hemifield ($R = -0.813$), the superotemporal quadrant ($R = -0.847$), the inferotemporal quadrant ($R = -0.855$), and the field sector representing the papillomacular bundle ($R = -0.809$). Coefficients of determination improved significantly in all sectors when time since surgery was included in the regression model—most notably, average thickness and 1/L ($R^2 = 0.35–0.49$), the decibels ($R^2 = 0.31–0.47$), and the temporal sector ($R^2 = 0.44–0.57$).

Conclusions. This is the first study to compare the structure–function correlation of RNFL measured by OCT with SAP in patients with chiasmal compression. RNFL is topographically related globally and sectorally to decreased SAP, with the temporal sectors showing the strongest correlations. The correlation between RNFL and VFS strengthens as the time from surgical intervention increases. (*Invest Ophthalmol Vis Sci.* 2006;47:4827–4835) DOI:10.1167/iovs.06-0327

From the [1]Neuro-ophthalmology Service, Department of Ophthalmology, and the [4]Clinical Trials Research Unit, School of Population Health, University of Auckland, Auckland, New Zealand; the [2]Neuro-ophthalmology Unit, Cullen Eye Institute, University of Baylor, Houston, Texas; and the [3]Neuro-ophthalmogy Service, Wills Eye Hospital, Philadelphia, Pennsylvania.

Supported by an unrestricted grant by Alcon Labs NZ.

Submitted for publication March 27, 2006; revised May 13 and June 13, 2006; accepted September 5, 2006.

Disclosure: **H.V. Danesh-Meyer**, None; **S.C. Carroll**, Alcon Labs NZ (F); **R. Foroozan**, None; **P.J. Savino**, None; **J. Fan**, None; **Y. Jiang**, None; **S. Vander Hoorn**, None

The publication costs of this article were defrayed in part by page charge payment. This article must therefore be marked "*advertisement*" in accordance with 18 U.S.C. §1734 solely to indicate this fact.

Corresponding author: Helen V. Danesh-Meyer, Department of Ophthalmology, Private Bag 92019, University of Auckland, Auckland, New Zealand; h.daneshmeyer@auckland.ac.nz.

Clinical assessment of optic neuropathies involves psychophysical assessment of optic nerve function with visual field (VF) tests and structural evaluation of the optic nerve head (ONH). Achromatic standard automated perimetry (SAP) is the gold standard for quantitatively evaluating visual field sensitivity (VFS). However, there is no validated method for quantifying optic nerve structure in nonglaucomatous optic neuropathies. The ONH is typically evaluated by grading the degree of optic disc pallor and assessing the retinal nerve fiber layer (RNFL), either with slit lamp fundus examination using red-free light or analysis of red-free RNFL photographs. These techniques require observer experience, are highly subjective, and are not readily quantified.[1] Because optic nerve function, but not structure, can be quantified in nonglaucomatous optic neuropathies, there is a paucity of data correlating alterations in VFS with changes in optic nerve morphology. This deficit limits the usefulness of ONH and RNFL assessment in evaluating and managing disease.

The situation is different with glaucomatous optic neuropathy, for which there is a large body of evidence supporting a specific anatomic correspondence between the pattern of ONH and RNFL thinning and VF defects.[2–8] Optical coherence tomography (OCT, StratusOCT; Carl Zeiss Ophthalmic Systems, Inc., Humphrey Division, Dublin, CA) has been shown to image and measure RNFL thickness in glaucomatous optic neuropathy and shows a strong spatial correlation with VFS.[9–11]

The relationship identified between glaucomatous optic neuropathy and VFS cannot be extrapolated to other optic neuropathies. Nonglaucomatous optic neuropathies cause a different pattern of clinical defects, for example, loss of central visual acuity, impaired color vision, and a much wider spectrum of VF defects. The morphologic changes identified in the optic nerve are also different. The hallmark of glaucoma is excavation of the optic cup and preservation of the remaining neuroretinal rim, without pallor, while nonglaucomatous optic neuropathies produce pallor of the neuroretinal rim. Finally, glaucomatous optic neuropathy is usually irreversible, whereas many optic neuropathies, particularly compressive optic neuropathies, may produce profound defects in visual function that are reversible after treatment.

The purpose of this study was to investigate the spatial correlation between loss of VFS (measured with SAP) and focal RNFL thinning (measured with OCT) in chiasmal compression, a type of compressive optic neuropathy. OCT was used because of its ability to provide high-resolution quantitative measurements of the RNFL in a clock-hour distribution.

Methods

Subjects

Twenty-six eyes from 26 patients with chiasmal compression, confirmed by neuroimaging, were recruited in the study from three sites (17 from Auckland City Hospital, Auckland, New Zealand; 8 from

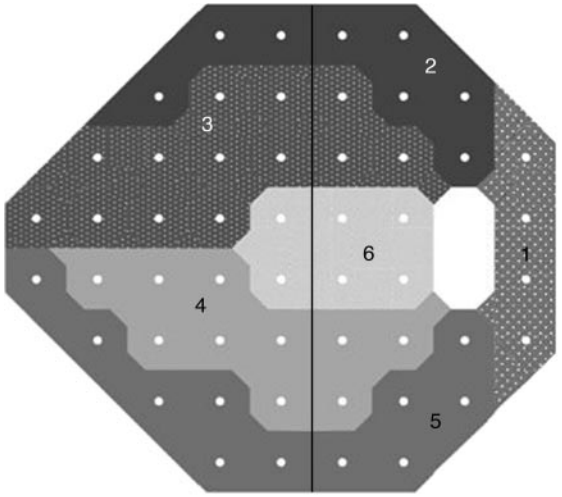

FIGURE 1. A division of the 24 VF test points and the optic nerve head into sectors, as suggested by Garway-Heath et al. The *vertical line* indicates where field sectors were divided along the vertical meridian (diagram for right VF and optic disc). Image reprinted from *Ophthalmology*, 107, Garway-Heath DF, Poinoosawmy D, Fitzke FW, Hitchings RA, Mapping the VF to the optic disc in normal tension glaucoma eyes, 1809–1815, © 2000, with permission from the American Academy of Ophthalmology.

Cullen Eye Institute, Houston, TX; and 1 from Wills Eye Hospital, Philadelphia, PA). For each subject, the eye with the more reliable VF indices (fewest false positives, false negatives, and fixation losses) was included in the study ($n = 26$). All patients had magnetic resonance imaging (MRI) of the brain that confirmed a lesion compressing the optic chiasm with the following diagnoses: 20 pituitary adenomas, 2 craniopharyngioma, 2 suprasellar meningioma, 1 chiasmal pilocytic astrocytoma, and 1 hypothalamic astrocytoma. The research adhered to the tenets of the Declaration of Helsinki. The institutional review committees had approved the research and informed consent had been obtained.

All patients underwent a complete ophthalmic examination, including visual acuity, refraction, slit lamp biomicroscopy, gonioscopy, intraocular pressure (IOP) measurement with Goldmann tonometry, and dilated stereoscopic fundus examination. Patients were not excluded on the basis of their visual acuity, but all patients were required to be able to perform reliable VF testing. All patients had a spherical refractive error within the range of ± 5 D and IOP measurement of less than 21 mm Hg. Patients were excluded if they any had anterior segment, retinal, posterior segment, or optic nerve disease other than compressive optic neuropathy. Specifically, patients with known glaucoma, family history of glaucoma, or cup-to-disc ratio asymmetry of greater than 0.2, focal notching, or optic nerve hemorrhage were excluded. Patients were also excluded from the study if they had a history of diabetes or any other systemic illness that may affect the retina and optic nerve. All subjects were a minimum of 3 months after surgery, radiotherapy, or chemotherapy.

Optical Coherence Tomography

Quantitative RNFL measurements were obtained using the StratusOCT (software version 3.0.1; Carl Zeiss Meditec, Inc.). The optical principles and applications of the OCT have been described in detail elsewhere.[12] The software outputs discrete RNFL thickness for each clock-hour position of the optic nerve head (for right eyes: 12 o'clock superiorly, 3 o'clock nasally, 6 o'clock inferiorly, and 9 o'clock temporally) and for each quadrant of the optic nerve head (superior: 11, 12, and 1 o'clock; nasal: 2, 3, and 4 o'clock; inferior: 5, 6, and 7 o'clock; and temporal: 8, 9 ,and 10 o'clock). The average RNFL thickness for the entire circumference is also provided. All data are displayed in right eye format, as just defined.

Procedure

The fast RNFL thickness (3.4) scan (100 scan points) acquisition protocol was used. Repeated measurements were taken by expert operators at each of the centers until three measurements judged to be of good quality were achieved for each eye. The RNFL thicknesses of the three scans were averaged internally to provide mean measurement for each clock hour position around the optic disc. For each clock hour, the investigators classified RNFL thickness measures as outside normal limits if they were thinner than 97.5% of normal values derived from an age-matched normative database (i.e., in the lowest 2.5 percentile) of 100 patients.[13] This cutoff was chosen to be conservative and to be consistent with other studies comparing structure- function.[6]

Standard Automated Perimetry

Standard automated perimetry was conducted using the Swedish Interactive Threshold Algorithm (SITA) 24-2 of the Humphrey Field Analyzer program (Carl Zeiss Meditec) with a Goldmann size III stimulus on a 31.5-apostilb background. Perimetry was performed within 2 weeks of OCT testing. All VFs included in the study had reliability indices of less than 33% false positives, false negatives, or fixation losses. The primary analysis involved dividing the VF data into nasal and temporal hemifields and further into superotemporal, inferotemporal, superonasal, and inferonasal quadrants. In another analysis, the VF data was divided into six sectors derived from a previously published optic disc-VF map. This latter analysis was particularly useful in that it allowed an evaluation of the relationship between the papillomacular fibers in the temporal optic disc with the corresponding central VF.[6] These sectors were further subdivided to allow analysis based on division along the vertical meridian (Fig. 1).

VF quadrants were defined as being outside normal limits if a minimum of two non–edge-contiguous test points, not including those directly above and below the blind spot, had a pattern deviation (PD plot) of one point with $P < 0.5\%$ and one point with $P < 2\%$. The cluster criteria for an abnormal hemifield (split into temporal and nasal hemifields) was three or more significantly depressed ($P < 5\%$) non–edge-contiguous points on the PD plot, with two of these points $P < 2\%$, not including those directly above and below the blind spot. Differential light sensitivity at each tested location is measured in decibels, where the differential light sensitivity (dB) $= 10 \cdot \log_{10} [L_{max}/(L_t - L_b)]$, where L_{max} is the maximum stimulus luminance, L_t is the stimulus luminance at threshold, and L_b is the background luminance. The unlogged 1/L at each test location was calculated by dividing the decibel unit by 10 and then unlogging it.

Statistical Analysis

Spearman's correlation coefficients and linear regression analyses were conducted to compare OCT-measured RNFL thickness deviation from normal age-adjusted RNFL thickness (in micrometers) to corresponding VF sectors. VF sensitivity was treated as the dependent variable and RNFL thickness as the independent variable in all regressions assessing the relationship between VFS and RNFL thickness. For further analysis, the structure–function relationship between average sectoral RNFL thickness and each VF zone was investigated using the raw VFS data

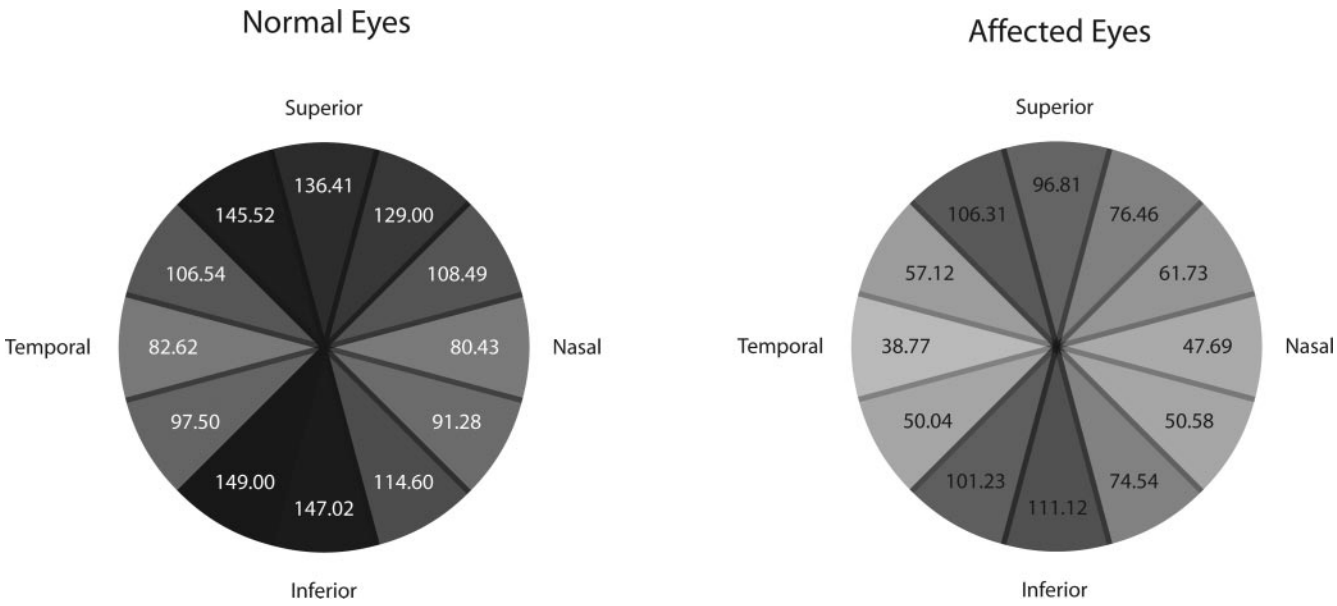

FIGURE 2. Diagrammatic representation of OCT RNFL thickness comparing normal eyes to affected eyes. *Grayscale* area uses the thickest area of RNFL as the reference (149 μm is 100% *black*; thus darker areas indicate a thicker RNFL). The diagram is for the right eye.

(not including blind spot points). The relationship between RNFL thickness and VF sensitivity was calculated for the whole field and field sectors (with their corresponding RNFL zones according to VF map) using linear and logarithmic regression analysis for both dB and 1/L scales (dB values are a logarithmic transform of differential light sensitivity [DLS]). All analyses were then repeated by including "time since surgery" in a multivariate regression model adjusting for age, sex and time since surgical intervention. A test for deviation from linearity was achieved by fitting a generalized additive model (GAM) and comparing to that of a linear model. Evidence of nonlinearity was assessed with a significance level of 0.05.

A paired *t*-test was performed to evaluate the null hypothesis that the absolute prediction errors (absolute values of the residuals) have the same mean for both models (linear and logarithmic regressions). Significance was assumed at $P < 0.05$. The linearity of the relationship between VF sensitivity and RNFL thickness was assessed by plotting the residuals of the linear regression against RNFL thickness.

RESULTS

Twenty-six eyes from 26 patients were included in the analysis, with a mean age of 41.1 ± 19.9 years (range, 8–73). There was an equal distribution of gender (13 male, 13 female). Subjects were studied a mean of 3.2 ± 3.6 years (range, 0.25–15.0) after surgery. Mean visual acuity was 6/9 with a range of 6/5 to 6/60, and a median logMAR (logarithm of the minimum angle of resolution) of 0.1. The mean percentage of correctly identified Ishihara color plates was 81% (range, 0%–100%).

OCT Results

The mean average thickness, a global measure of RNFL thickness, was 72.66 ± 19.24 μm (compared with normal controls 115.91 ± 14.29 μm; $P < 0.0001$). Figure 2 diagrammatically displays the absolute thickness of RNFL in micrometers, comparing normal eyes ($n = 100$) to affected eyes ($n = 26$). For all clock hours the RNFL was significantly thinner ($P < 0.0001$ in all cases) in affected eyes than controls. Figure 3 shows the percentage of RNFL loss for each clock hour. When the clock hours were combined to form four quadrants (superior, inferior, nasal, and temporal), it was clear that the temporal and nasal disc sectors demonstrated a significantly greater proportion of thinning that did the superior and inferior disc sectors (50% and 42% vs. 32% and 31% thickness loss, respectively; $P < 0.001$). Twenty-one (81%) of 26 eyes were >2 SD below normal, representing a 38% loss of thickness. The temporal (77% of eyes abnormal) and nasal (65%) sectors of the disc were more frequently abnormal than were the superior (62%) and inferior sectors (54%). The most frequently abnormal clock hours of RNFL thickness were 9 o'clock (69%, representing the temporal pole of the disc) and the adjacent 10 o'clock (65%) and 8 o'clock (62%) positions. In summary, although there was generalized thinning of all sectors of the RNFL, the temporal and nasal sectors displayed the most marked loss of RNFL.

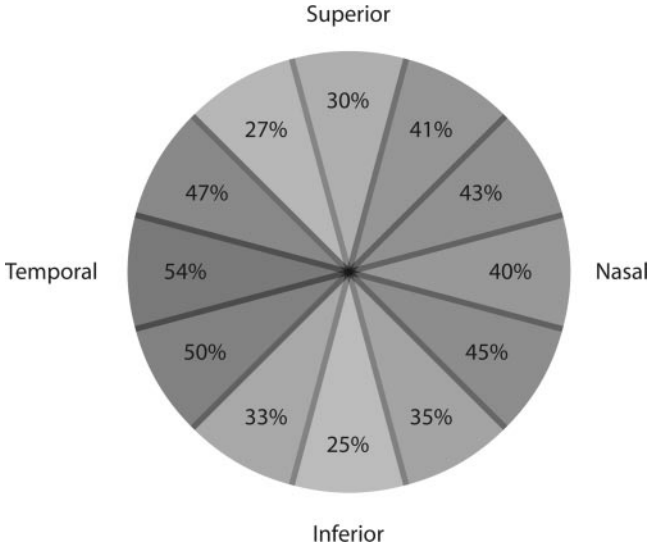

FIGURE 3. The percentage of OCT RNFL thickness lost, when compared to normative data. *Darker shading* indicates a greater percentage of thickness lost (*white*, 0% thickness lost; *black,* 100% thickness lost).

TABLE 1. Proportion of Eyes Outside Normal Limits and Mean PD in Decibels for VF Zones

Visual Field Zones	Eyes Outside Normal Limits, *n* (%)	Mean PD (SD) (dB)
Temporal hemifield	24 (92)	−12.93 (9.85)
Superotemporal quadrant	23 (88)	−14.42 (9.51)
Inferotemporal quadrant	20 (77)	−11.92 (11.36)
Nasal Hemifield	3 (11)	−2.31 (2.18)
Superonasal quadrant	2 (8)	−2.12 (3.68)
Inferonasal quadrant	1 (4)	−2.16 (1.47)
VF Sector 1 (entirely temporal)	—	−15.14 (11.12)
VF Sector 2	—	−9.74 (6.41)
Temporal half	—	−13.77 (9.54)
Nasal half	—	−3.03 (3.61)
VF Sector 3	—	−4.75 (2.33)
Temporal half	—	−14.14 (9.20)
Nasal half	—	−1.93 (1.31)
VF Sector 4	—	−4.87 (5.22)
Temporal half	—	−11.23 (12.44)
Nasal half	—	−2.15 (3.90)
VF Sector 5	—	−5.90 (5.89)
Temporal half	—	−10.69 (11.63)
Nasal half	—	−1.90 (3.46)
VF Sector 6	—	−10.37 (8.39)
Temporal half	—	−14.27 (12.03)
Nasal half	—	−2.56 (2.65)

VF Results

The mean Humphrey visual field (HVF) mean deviation (MD) for the study group was −9.62 ± 6.96 dB (range, −1.04 to −25.29). The mean HVF PSD was 8.44 ± 5.30 (range, 1.48 to −17.03) The proportion of eyes with field sectors outside normal limits and the mean PSD for these sectors are shown in Table 1. The temporal VF zones were more significantly depressed and more frequently outside normal limits than were the nasal zones in every instance ($P < 0.0001$). The most depressed VF quadrant was the superotemporal one. The two VF areas that demonstrated the greatest loss of VF sensitivity when the VF was divided into sectors according to the VF map (Fig. 1), were sector 1 (the four most temporal points of the VF) with a mean PSD of −15.14 dB (corresponding to the nasal disc sector), and the temporal part of sector 6 (corresponding to the papillomacular bundle) with a mean PSD of −14.27 dB.

Correlation between RNFL Thickness and VFS

The deviation from normal RNFL thickness showed strong correlations with the temporal VF sectors (Table 2). The four strongest correlations were at the 8 o'clock OCT position (temporal disc), in the temporal hemifield ($R = -0.813$, $P < 0.00001$), the superotemporal quadrant ($R = -0.847$, $P < 0.00001$), the inferotemporal quadrant ($R = -0.855$, $P < 0.00001$), and the papillomacular bundle ($R = -0.809$, $P < 0.00001$). In general, the superotemporal sector yielded higher correlation coefficients than the inferotemporal sector. Nasal field sectors were not significantly correlated with OCT parameters. When nonquadrant

TABLE 2. Relationship between OCT RNFL Deviation from Normal for Each OCT Parameter and Average Visual Field PSD at Each Visual Field Zone

OCT Parameter	MD	PSD	T	ST	IT	N	SN	IN	Central Visual Field (temporal to vertical meridian)
S	**−0.47**	**0.59**	**−0.65**	**−0.63**	**−0.59**	−0.30	−0.09	−0.13	**−0.56**
N	−0.14	0.41	−0.40	−0.45	−0.30	−0.15	−0.11	0.11	−0.24
I	−0.24	0.40	−0.35	**−0.40**	−0.32	−0.26	−0.12	−0.05	−0.26
T	**−0.58**	**0.74**	**−0.77**	**−0.77**	**−0.64**	−0.30	−0.09	0.01	**−0.75**
Average thickness	**−0.41**	**0.62**	**−0.63**	**−0.64**	**−0.53**	−0.28	−0.07	−0.15	**−0.49**
OCT.01 (S)	**−0.32**	**0.56**	**−0.61**	**−0.58**	**−0.55**	−0.12	0.09	−0.13	**−0.48**
OCT.02 (N)	−0.36	**0.54**	**−0.57**	**−0.60**	**−0.46**	−0.35	−0.17	−0.01	−0.38
OCT.03 (N)	0.02	0.28	−0.24	−0.30	−0.18	−0.08	−0.08	0.13	−0.13
OCT.04 (N)	−0.04	0.20	−0.17	−0.20	−0.13	−0.03	−0.07	0.04	−0.05
OCT.05 (I)	−0.16	0.22	−0.21	−0.22	−0.20	−0.27	0.08	−0.05	−0.08
OCT.06 (I)	−0.12	0.20	−0.16	−0.15	−0.14	−0.25	−0.24	−0.05	−0.01
OCT.07 (I)	**−0.37**	**0.55**	**−0.51**	**−0.59**	−0.41	−0.30	−0.04	−0.12	**−0.50**
OCT.08 (T)	**−0.62**	**0.81**	**−0.86**	**−0.85**	**−0.73**	−0.20	0.10	−0.07	**−0.80**
OCT.09 (T)	**−0.46**	**0.67**	**−0.71**	**−0.70**	**−0.57**	−0.17	−0.01	0.11	**−0.65**
OCT.10 (T)	**−0.52**	**0.58**	**−0.61**	**−0.60**	**−0.52**	−0.37	−0.23	0.01	**−0.62**
OCT.11 (S)	**−0.47**	**0.47**	**−0.49**	**−0.51**	**−0.46**	−0.33	−0.19	−0.01	**−0.50**
OCT.12 (S)	**−0.43**	**0.55**	**−0.60**	**−0.55**	**−0.60**	−0.22	−0.07	−0.11	**−0.49**

Data are the Spearman correlation coefficient. Bold results, $P < 0.05$, bold and underscored, $P < 0.001$ (subanalysis of visual field zones split into temporal and nasal halves not shown in entirety). S, superior; I, inferior; T, Temporal; N, Nasal; ST, superotemporal; IT, inferotemporal; SN, superonasal; IN, inferonasal; Avg, average.

TABLE 3. Coefficient of Determination (R^2) of Regression between VFS (Raw Sensitivity Data) and RNFL Thickness, without and with "Time since Surgery" Incorporated into the Analysis

Without Time since Surgery

	dB Sensitivity			1/L Sensitivity		
OCT Parameter (Clock Hour)	**Linear Regression (R^2)**	**Logarithmic Regression (R^2)**	**Difference in Fit (P)**	**Linear Regression (R^2)**	**Logarithmic Regression (R^2)**	**Difference in Fit (P)**
Avg. thick	0.31	0.31	0.401	0.35	0.31	0.018
OCT.09	0.17	0.17	0.304	0.29	0.28	0.886
T	0.34	0.33	0.456	0.44	0.40	0.291
OCT.03	0.12	0.12	0.864	0.05	0.06	0.658
N	0.18	0.18	0.316	0.10	0.11	0.490
I	0.22	0.21	0.440	0.22	0.17	0.100
S	0.39	0.41	0.211	0.32	0.29	0.100

With Time since Surgery

	dB Sensitivity			1/L Sensitivity		
OCT Parameter (Clock Hour)	**Linear Regression (R^2)**	**Logarithmic Regression (R^2)**	**Difference in Fit (P)**	**Linear Regression (R^2)**	**Logarithmic Regression (R^2)**	**Difference in Fit (P)**
Avg. thick.	0.47	0.46	0.360	0.49	0.46	0.020
OCT.09	0.27	0.27	0.960	0.40	0.39	0.759
T	0.46	0.45	0.844	0.57	0.53	0.125
OCT.03	0.18	0.19	0.286	0.07	0.08	0.471
N	0.24	0.26	0.294	0.12	0.13	0.857
I	0.31	0.32	0.796	0.55	0.55	0.373
S	0.53	0.55	0.422	0.52	0.48	0.037

Avg. thick, average thickness; S, superior; I, inferior; T, temporal.

VF sectors based on the VF map were divided into subsectors by the vertical meridian, the temporal subdivisions matched the magnitude and significance of the relationships in the undivided sectors, whereas nasal subdivisions were nonsignificant.

Global and sectoral relationships between raw VF sensitivity (in dB and 1/L units) and RNFL thickness were analyzed using linear and logarithmic regression for both scales. Coefficients of determination (R^2) for these analyzes are summarized in Table 3. The strongest sectoral R^2 was observed in the temporal OCT sector and the corresponding central part of the VF ($R^2 = 0.44$) using the 1/L scale with linear regression. When the analyses included time since surgery in the regression model, the coefficients of determination improved significantly in both the 1/L linear regressions (from 0.35 to 0.49 for average thickness), and the dB linear regressions (from 0.31–0.47) and with the temporal sector strengthening ($R^2 = 0.57$).

Table 4 shows the slopes of RNFL thickness loss versus VF sensitivity loss in both the dB and 1/L scale with the values standardized such that the *x*-axis (OCT RNFL thickness) is $X = (X - \text{mean } [X])/\text{SD } (Y)$ and the *y*-axis (VF sensitivity) is $Y = (X - \text{mean } [X])/\text{SD } (X)$. This normalization of OCT and VF parameters allowed direct comparison of slopes between different field sectors and RNFL measures. The steepest slope (0.67) was in the central VF (VF sector 6) and the corresponding temporal optic disc (papillomacular bundle). The shallowest slope was in the inferonasal quadrant and the corresponding superior optic disc (0.23). The remainder of slopes ranged from 0.31 to 0.63. In general, those slopes associated with the temporal disc and corresponding VF sectors were steeper than those associated with the nasal disc and their corresponding VF sectors (0.40–0.67 vs. 0.23–0.34).

The relationship between RNFL and VA or color vision was also studied. All patients who had VA of 20/30 or worse had temporal disc RNFL thickness of 50 μm or less. A similar relationship was seen with Ishihara color plate performance,

TABLE 4. Slopes and 95% Prediction Intervals of Slope for Relationship between VF Sensitivity and RNFL Thickness

Visual Field Zone	Slope for 1/L Sensitivity (95% CI for slopes)	Slope for dB Sensitivity (95% CI for slopes)
Mean VFS	0.63 (0.32–0.94)	0.60 (0.28–0.91)
Visual field sector 6	0.67 (0.39–0.95)	0.60 (0.28–0.91)
Visual field sector 1	0.34 (0.07–0.75)	0.47 (0.09–0.84)
Superotemporal	0.47 (0.10–0.85)	0.47 (0.10–0.85)
Superonasal	0.31 (0.02–0.60)	0.24 (0.02–0.60)
Inferotemporal	0.40 (0.31–0.90)	0.45 (0.36–0.95)
Inferonasal	0.23 (0.13–0.59)	0.36 (0.02–0.74)

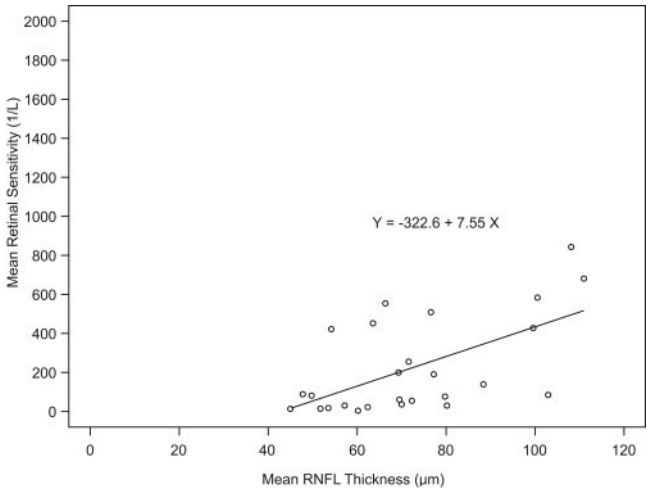

FIGURE 4. Scatterplot of Average RNFL thickness measured by OCT and VFS in the 1/L scale.

where every subject who incorrectly identified 3 or more of 14 color plates had temporal disc RNFL thickness below 50 μm.

A scatterplot of raw VFS in 1/L scale (Fig. 4) against mean RNFL thickness reveals an offset bias of RNFL measurements with no readings below approximately 40 μm. A scatterplot of the relationship between temporal disc RNFL thickness and the corresponding VFS of the papillomacular bundle (VF sector 6) showed that there was a change in the structure–function relationship at a value of 50 μm (Fig. 5). Below this RNFL thickness, the VFS showed marked variability; however, when the thickness was more than 50 μm, the relationship was more predictable.

DISCUSSION

This is the first study to compare the structure-function correlation of RNFL thinning, as measured by OCT with SAP in patients with chiasmal compression. Our data demonstrated that loss of RNFL thickness correlated with the severity of loss of VFS and occurred diffusely in all sectors, even in patients who had strict bitemporal hemianopic VF loss on SAP. However, the horizontal sectors of the RNFL (temporal and nasal) showed proportionately greater thinning than did vertical sectors, consistent with the clinical appearance of "band atrophy" that may be seen in patients with chiasmal compression. The correlation between RNFL and VFS strengthened as the time from surgical intervention increased. The sectoral correlations showed patterns distinctively different from glaucoma, with the temporal optic disc showing the strongest correlation with the corresponding central VF as well as with central visual acuity and color vision.

These findings extend our understanding of distribution of RNFL loss at the optic nerve head when the site of damage is at the chiasm. The two available histopatholgic examinations of the optic nerve in patients with optic atrophy secondary to chiasmal compression[14,15] suggest that this syndrome leads to severe atrophy of temporal and nasal fibers that originate from ganglion cells nasal to the fovea. Our results also showed temporal and nasal loss of the RNFL, but in addition, diffuse loss over the entire disc. The diffuse loss of RNFL reflects that in most cases, although compressive lesions of the chiasm primarily affect the crossing fibers, they also affect noncrossing fibers.[16] Three smaller studies have also demonstrated diffuse thinning of the RNFL in chiasmal compression using OCT and scanning laser polarimetry (SLP), in addition to preferential thinning of the temporal and nasal sectors.[17–19]

The clinical diagnosis of optic atrophy is based on pallor of the optic disc, narrowing of the retinal vasculature, and loss of RNFL reflexes. The evaluation of optic disc color is subjective and of unproven reliability. Furthermore, it is well recognized that the degree of pallor does not necessarily correlate with the level of visual function. Several investigators have evaluated methods for improving the grading of optic pallor including enlarging high-contrast black and white prints,[20,21] estimating optic atrophy by color contrast, and quantifying the degree of atrophy by microdensity in the blue (470 nm) and in the red (640 nm) regions.[22,23] Focal loss of the RNFL may be visualized as retinal nerve fiber bundle defects.[24] However, these techniques require methods unavailable in standard clinical practice and demand a high degree of familiarity with the techniques. OCT appears to provide a more objective and practical measurement of RNFL loss than does clinical assessment.

Our OCT measurements of the RNFL provide an accurate reflection of the degree of VF loss. The present study had a good range (MD from −1.04 to −25.29) of normal to severe VF for study and therefore is able to represent a comparison of OCT and VF effectively. The correlations between VF loss and RNFL were robust in that the temporal areas that demonstrated significant field loss correlated highly with OCT thinning, whereas the nasal VF sectors did not show significant correlations with corresponding VF zones.

This study allows the first comparison of structure–function relationships between glaucoma and another disease in which retinal ganglion cells are the primary neuron that is injured. The quantitative comparison between functional and structural deficits in the same eye has been evaluated to date solely in normal and glaucomatous eyes. Glaucomatous optic neuropathy has been shown to produce loss of VFS that correlates both in extent and location to OCT-identified areas of RNFL thinning.[25–27] Reasonably strong global correlations have been shown between mean RNFL thickness and SAP or corrected PSD (R = 0.68 and −0.59, respectively).[28] Clinically, glaucomatous optic neuropathy is characterized by preferential loss of RNFL in an hour-glass pattern, loss superiorly and inferiorly, with relative sparing of the temporal and nasal sectors.[29] Quantitatively, OCT-measured thinning of superior and inferior RNFL correlates with SAP MD, inferior SAP sensitivity, and superior SAP sensitivity at R^2 = 0.35, 0.38, and 0.43, respectively.[25] Studies in glaucoma have consistently shown that the

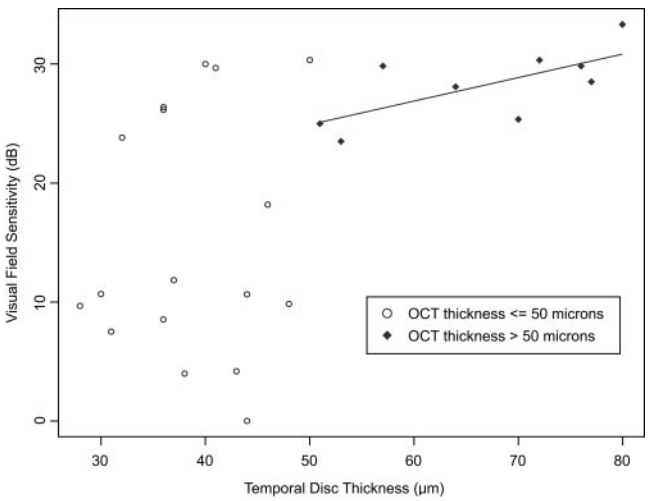

FIGURE 5. Scatterplot of temporal OCT RNFL thickness measured by OCT and VFS in the papillomacular bundle (VF sector 6).

superior and inferior structural analyses by sector were more informative in predicting VF loss than data from the temporal or nasal sectors and correlate more strongly with the corresponding VF sectors.[3,30,31]

In contrast, the present study has demonstrated that chiasmal compression has a different pattern of regional OCT loss and corresponding VF damage from that of glaucoma. Although retinal ganglion cells die diffusely in both conditions, chiasmal injury causes greater injury in the temporal and nasal RNFL and strong correlations between structure and function in the corresponding VF sectors. Patients with chiasmal syndrome have, in addition, correlations between temporal RNFL thickness loss and visual acuity and color vision. The differences between glaucoma and chiasmal syndromes effect on retinal ganglion cells may derive from the location of injury to their axons, the type of injury, or its chronicity. Current evidence suggests that the major site of damage in glaucoma is at the level of the optic nerve head/lamina cribrosa with the superior and inferior poles being the most susceptible sites. In chiasmal compression, the axons that are closest to the expanding mass are those crossing from the nasal hemiretinal ganglion cells. The temporal hemiretinal fibers become involved when the tumor enlarges and affects the noncrossing fibers. The mechanism of injury may also partly explain the difference between compression and glaucoma; the slow chronic nature of compression by the tumor may result in axoplasmic stasis compared with glaucoma. Hence, this may reflect a reversibility that is not usually present in glaucoma.

The structure–function relationship tended to strengthen as time passed after the surgical intervention. Recovery of vision, both immediate and delayed, after decompression surgery is a well-established occurrence. Immediate recovery is postulated to result from the removal of physiologic conduction block and restoration of signal conduction.[32,33] Visually evoked potentials have been documented to occur within 10 minutes of decompression.[34] Delayed recovery of visual function after compression of the optic nerve has been attributed to progressive remyelination of previously compressed axons that have undergone demyelination or re-establishment of vascular supply that potentially is hampered by stretching of the chiasmal blood supply by the tumor and consequent improvement of retinal ganglion cell function.[33,35–39] As the interval from intervention increases, it is likely that the fate of the RGC is determined: Either the dysfunctional RGCs recover or they die. The relationship between structure and function strengthens as the component of RGCs that are damaged but not dead decreases. In other words, VF testing measures defects produced by both dead and dysfunctional RGCs, whereas anatomic measurements such us RNFL thickness only reflect the axons that have died. After the compression is relieved by surgical intervention, the VF improves for those axons that were nonfunctional, and the anatomic measurements reflect the surviving axons. This suggests that visual sensitivity losses likely precede ganglion cell death in compression syndromes and psychophysical measures in this setting include a component of cell dysfunction as well as cell death. Although this is striking in compression syndromes, this potential period of visual recovery has not been validated to occur in glaucoma. For example, detailed histologic analysis of retinal ganglion cell morphology after intracellular injection of fluorescent dyes has shown that the cell soma, dendritic tree, and axon may shrink before the onset of cell death in glaucoma.[40–42] This observation suggests that the potential may exist to predict which patients may demonstrate improvement of visual function in chiasmal compression: If RNFL thinning does not occur even in the presence of profound VF loss, it may be that visual recovery is possible.

In glaucomatous optic neuropathy, there is a linear relationship between the number of ganglion cells and DLS when DLS is represented in the 1/L scale.[43–45] This suggests that structural and functional damage follow a parallel path, despite the obvious variabilities in test paradigms. It is clear evidence that in glaucoma the methods for measuring reduction in the number of cells and loss of cell responsiveness are closely linked. The relationship is not linear when DLS is represented in the decibel scale, because this presents the information logarithmically transformed by comparison with nonlogarithmically plotted cell anatomic data. When we view the relationship in thickness versus decibel scales, the VF sensitivity changes at more normal decibel levels are minimal (compared to OCT thickness) and are magnified at low decibel levels.[44,45] We found that chiasmal compression also suggests a linear relationship for global index information, but the power of the study may have prevented confirming such a relationship sectorally. Despite differences between glaucoma and compression syndromes, the implication is that disorders in which ganglion cells die diffusely, as well as within their own selective patterns, lead to a consistent loss of functional capability for an increment of anatomic neuronal loss. In essence, this serves as a validation of both our structural and functional test methods.

There were differences, however, between the details of the structure–function correlation in compression compared with glaucoma. The slope of the structure–function regression models are different in compression and glaucoma (Schlottman et al.[7]). In part, difference may result from our method of normalization of OCT and VF parameters, because of the difference in variability of each parameter. This allows direct comparison of slopes between different field sectors and RNFL measures, but is not a method used in other studies. The same level of change in RNFL thickness at the papillomacular bundle results in greater change in VF sensitivity than any other sector of the RNFL. In glaucoma, it was the superotemporal and inferotemporal sectors that had the steepest slopes.[7] The differences in the slopes could be explained by preferential damage to different types of ganglion cells, their regional distribution, or the different time course of the disease process.

It is intriguing that some relationships that would be expected to be strong were not. For example, the nasal side of the disc did not show a stronger correlation to the corresponding temporal sectors. This finding may be in part due to the smaller range of VF defects in these sectors, as they tended all to be significantly abnormal. However, OCT clock hour 2 had a robust correlation to VF sector 1 of the Garway-Heath map (which are the four points exclusively temporal). Also, the nasal VF sectors did not show any significant correlation to the corresponding temporal optic disc sectors. Although we identified thinning in the superior and inferior RNFL of approximately 33%, the SITA-standard VF test identified only mild abnormalities in the corresponding nasal sectors with no nasal sector showing a mean deviation of greater than −4.8 dB.

Hence, the lack of correlation may be due to the limitation of white-on-white perimetry to identify early abnormalities in the VF. Studies have shown that short-wavelength automated perimetry and frequency doubling technology have shown closer agreement with structural assessments in glaucomatous optic neuropathy.[46] Further research comparing structural parameters with other psychophysical tests of visual function may also demonstrate stronger correlations for compressive optic neuropathies.

Alternatively, the generalized thinning of the RNFL may be explained by the fact that every clock hour of the optic disc receives crossing fibers; even the temporal side of the disc receives fibers from the retina between the vertical meridian through the fovea and the disc. The upper and lower poles of the optic disc receive a significant number of fibers from the

retina temporal to the fovea, which are noncrossing fibers, and this is why the loss of fibers in these sectors would not be expected to be as dramatic as in the bow-tie region, which receives predominantly crossing fibers.

There are several limitations of this study that may affect the accuracy of correlating clinical VFs with ganglion cell loss. Some are due to the inherent anatomic and psychophysiologic variability in the techniques used in measuring structure or function. At RNFL thicknesses below 50 μm (Fig. 5), there was tremendous variability in central VFS. We never measured RNFL thickness less than 40 μm. Schlottman et al.[7] were unable to measure RNFL less than 20 μm with SLP[7] and suggested that this inability may be due either to inaccuracies in measuring a thin RNFL or to other unspecified sources of retardation. It is possible that even with complete axonal loss, the residual nerve fiber layer measured by the OCT is a reflection of other structures such as astrocytes.

Some areas of the RNFL may have a higher interindividual variability than others. It has been suggested that the inferotemporal and superotemporal sectors have lower intereye variability in normal subjects.[47] Another sector-related problem could be the correlation between the RNFL thicknesses of adjacent sectors, causing relationships to appear with sectors that are merely close neighbors of the responsible sector resulting in the well-correlated areas appearing wider. Garway-Heath et al.[5] discussed that in devising their structure–function map, the mean SD of VF sectors for correspondence at the optic nerve head positions was 7.2°, suggesting that 95% of the time a VF test point will be associated with a position at the ONH within approximately 14° either side of a mean. Thus, the range of possible positions at the optic nerve covers almost 30° for each VF test point. Variability in the location of the OCT scan with regard to the disc margin may also reduce the strength of the relationship between deviation from normal RNFL thickness and SAP PD. Not surprisingly, the VF/optic nerve map used in this study failed to identify with certainty the structure–function correlation, as the map was derived from a cohort of patients with glaucoma. However, when the map was further subdivided to respect the vertical meridian, the correlation of the temporal Garway-Heath sectors were as robust as the hemifields and quadrants; because, although lesions in the chiasm result in anterograde degeneration, they do not alter the relationship between the loss of axons or the thinning of the RNFL at the optic disc and its associated retinal ganglion cell bodies. Finally, despite this study's being the largest series of compressive optic neuropathies quantified with OCT and SAP reported to date, the number of patients studied may have limited the identification of significant relationships. In summary, this study adds to the body of evidence for a topographic structure–function relationship in optic neuropathies. RNFL thinning and regional decreases in VF sensitivity are topographically related in both location and severity in compressive optic neuropathies, with the temporal optic disc having the strongest structure–function correlation. Because of the high correlation demonstrated between VFS and corresponding RNFL thickness, OCT may provide an objective measure of ganglion cell axonal loss in chiasmal compression and may have a useful role in the management of these conditions. Furthermore, the study clearly demonstrates a difference in the topographic changes identified at the optic nerve head between glaucoma, which results in RNFL thinning at the superior and inferior poles, and chiasmal compression, which shows greatest RNFL thinning at the temporal optic disc. This finding may be potentially useful clinically in cases in which both diagnoses are under consideration. However, further research is appropriate to determine the sensitivity and specificity of this association as measured by OCT. These findings should stimulate the investigation of whether the OCT RNFL measurement can serve as a prognostic indicator for the recovery of vision after decompressive surgery.

Acknowledgments

The authors thank Len Levin and Harry Quigley for their editorial review of the manuscript.

References

1. Quigley HA, Reacher M, Katz J, Strahman E, Gilbert D, Scott R. Quantitative grading of nerve fiber layer photographs. *Ophthalmology*. 1993;100:1800–1807.
2. Weinreb RN, Shakiba S, Sample PA, et al. Association between quantitative nerve fiber layer measurement and visual field loss in glaucoma. *Am J Ophthalmol*. 1995;120:732–738.
3. Iester M, Swindale N, Mikelberg F. Sector-based analysis of optic nerve head shape parameters and visual field indices in healthy and glaucomatous eyes. *J Glaucoma*. 1997;6:370–376.
4. Bosworth CF, Sample PA, Williams JM, et al. Spatial relationship of motion automated perimetry and optic disc topography in patients with glaucomatous optic neuropathy. *J Glaucoma*. 1999;8:281–289.
5. Garway-Heath DF, Poinoosawmy D, Fitzke FW, Hitchings RA. Mapping the visual field to the optic disc in normal tension glaucoma eyes. *Ophthalmology*. 2000;107:1809–1815.
6. El Beltagi TA, Bowd C, Boden C, et al. Retinal nerve fiber layer thickness measured with optical coherence tomography is related to visual function in glaucomatous eyes. *Ophthalmology*. 2003; 110:2185–2191.
7. Schlottman PG, De Cilla S, Greenfield DS, et al. Relationship between visual field sensitivity and retinal nerve fiber layer thickness as measured by scanning laser polarimetry. *Invest Ophthalmol Vis Sci*. 2004;45:1823–1829.
8. Reus NJ, Lemij HG. The relationship between standard automated perimetry and GDx VCC measurements. *Invest Ophthalmol Vis Sci*. 2004;45:840–845.
9. Huang D, Swanson EA, Lin CP, et al. Optical coherence tomography. *Science*. 1991;54:1178–1181.
10. Schuman JS, Hee MFR, Arya AV, et al. Optical coherence tomography: a new tool for glaucoma diagnosis. *Curr Opin Ophthalmol*. 1995;6:89–95.
11. Blumenthal EZ, Williams JM, Weinreb RN, et al. Reproducibility of nerve fiber layer thickness measurements by use of optical coherence tomography. *Ophthalmology*. 2000;107:2278–2282.
12. Schuman JS, Pedut-Kloizman T, Hertzmark E, et al. Reproducibility of nerve fiber layer thickness measurements by use of optical coherence tomography. *Ophthalmology*. 2000;103:1889–1898.
13. Bowd C, Zangwill LM, Blumenthal EZ, et al. Imaging of the optic disc and retinal nerve fiber layer: the effects of age, optic disc area, refractive error, and gender. *J Opt Soc Am A Opt Image Sci Vis*. 2002;19:197–207.
14. Hoyt WF. Fundoscopic changes in the retinal nerve fibre layer in chronic and acute optic neuropathies. *Trans Ophthalmol Soc UK*. 1976;96:368–371.
15. Unsold R, Hoyt WF. Band atrophy of the optic nerve. *Arch Ophthalmol*. 1980;98:1637.
16. Trobe JD, Tao AJ, Shuster JJ. Pre-chiasmal tumor: diagnostic and prognostic features. *Neurosurgery*. 1984;15:391–309.
17. Monteiro MLR, Medeiros FA, Ostroscki MR. Quantitative analysis of axonal loss in band atrophy of the optic nerve using scanning laser polarimetry. *Br J Ophthalmol*. 2003;87:32–37.
18. Monteiro MLR, Leal BC, Rosa AAM, Bronstein MD. Optical coherence tomography analysis of axonal loss in band atrophy of the optic nerve. *Br J Ophthalmol*. 2004;88:896–899.
19. Kanamori A, Nakamura M, Matsui N, et al. Optical coherence tomography detects characteristic retinal nerve fiber layer thickness corresponding to band atrophy of the optic discs. *Ophthalmology*. 2004;111:2278–2283.
20. Schwartz B, Reinstein NM, Lieberman DM. Pallor of the optic disc; quantitative photographic evaluation. *Arch Ophthalmol*. 1973;89: 278–286.

21. Berkowitz JS, Balter S. Colorimetric measurement of the optic disc. *Am J Ophthalmol*. 1970;69:385–386.
22. Sorenson PH. The pallor of the optic disc: a quantitative photographic assessment by purple filter. *Acta Ophthalmol*. 1979;57: 718–724.
23. Davies EWG. Quantitative assessment of colour of the optic disc by photographic method. *Exp Eye Res*. 1970;9:106–113.
24. Hoyt WF, Schlicke B, Eckelhoff RJ. Funduscopic appearance of a nerve fibre bundle defect. *Br J Ophthalmol*. 1972;56:577–583.
25. Zangwill LM, Williams J, Berry CC, et al. A comparison of optical coherence tomography and retinal nerve fiber layer photography for detection of nerve fiber layer damage in glaucoma. *Ophthalmology*. 2000;107:1309–1315.
26. Schuman JS, Hee MR, Puliafito CA, et al. Quantification of nerve fiber layer thickness in normal and glaucomatous eyes using optical coherence tomography. *Arch Ophthalmol*. 1995;113:586–596.
27. Pieroth L, Schuman JS, Hertzmark E, et al. Evaluation of focal defects of the nerve fiber layer using optical coherence tomography. *Ophthalmology*. 1999:570–579.
28. Hoh ST, Greenfield DS, Mistlberger A, et al. Optical coherence tomography and scanning laser polarimetry in normal, ocular hypertensive, and glaucomatous eyes. *Am J Ophthalmol*. 2000:129–135.
29. Quigley HA, Miller NR, Green R. The pattern of optic nerve fiber loss in anterior ischemic optic neuropathy. *Am J Ophthalmology*. 1985;100:769–776.
30. Gundersen K, Heijl A, Bengtsson B. Optic nerve head sector analysis recognizes glaucoma most effectively around disc poles. *Acta Ophthalmol Scand*. 1999;77:13–18.
31. Emdadi A, Kono Y, Sample P, Maskaleris G, Weinreb R. Parapapillary atrophy in patients with focal visual field loss. *Am J Ophthalmol*. 1999;128:595–600.
32. Cushing H, Walker CB. Distortion of the visual fields in cases of brain tumor. IV Chiasmal lesions with special reference to bitemporal hemianopia. *Brain.* 1915:371–400.
33. Kayan A, Earl CJ. Compressive lesions of the optic nerves and chiasm, pattern of recovery of vision following surgical treatment. *Brain*. 1975;98:13–28.
34. Feinsod M, Selhorst JB, Hoyt WF, Wilson CB. Monitoring optic nerve function during craniotomy. *J Neurosurg*. 1976;44:29–31.
35. Harrison BM, McDonald WI. Remyelination after transient experimental compression of the spinal cord. *Ann Neurol*. 1977;1:552–560.
36. Jacobson SG, Eames RA, McDonald WI. Optic nerve fiber lesions in adult cats: pattern of recovery of spatial vision. *Exp Brain Res*. 1979;36:491–508.
37. McDonald WI. The 1981 Silversides Lecture. The symptomology of tumours of the anterior visual pathways. *Can J Neurol Sci*. 1982; 9:381–390.
38. Kerrison JB, Lynn MJ, Baer CA, et al. Stages of improvement in visual fields after pituitary tumor resection. *Am J Ophthalmol*. 2000;130:813–820.
39. Clifford-Jones RE, Landon DN, McDonald WI. Demyelination during optic nerve compression. *J Neurol Sci*. 1980;46:37–40.
40. Weber AJ, Kaufman P, Hubbard WC. Morphology of single ganglion cells in the glaucomatous primate retina. *Invest Ophthalmol Vis Sci*. 1998;39:2304–2320.
41. Morgan JE, Uchida H, Caprioli J. Retinal ganglion cell death in experimental glaucoma. *Br J Ophthalmol*. 2000;84:303–310.
42. Morgan JE. Selective cell loss in glaucoma: does it really occur? *Br J Ophthalmol*. 1994;78:875–880.
43. Garway-Heath DF, Viswanathan A, Westcott M, Kamal D, Fritzke FW, Hitchings RA. Relationship between perimetric light sensitivity and optic disc neuroretinal rim area. In: Wall M, Wild JM, eds. *Perimetry Update*. The Hague, The Netherlands: Kugler Publications; 1998/1999;381–389.
44. Jonas JB, Grundler AE. Correlation between mean visual field loss and morphometric optic disk variables in the open-angle glaucomas. *Am J Ophthalmol*. 1997;124:488–497.
45. Garway-Heath DF, Holder GE, Fitzke FW, Hitchings RA. Scaling the hill of vision: the physiological relationship between ganglion cells numbers and light sensitivity. *Invest Ophthalmol Vis Sci*. 2000;41: 1774–1782.
46. Bagga H. Feuer WJ, Greenfield DS. Detection of psychophysical and structural injury in eyes with glaucomatous optic neuropathy and normal standard automated perimetry. *Arch Ophthalmol.* 2006;24:169–176.
47. Garway-Heath DF, Hitchings R. Quantitative evaluation of the optic nerve head in early glaucoma. *Br J Ophthalmol*. 1998;82: 352–361.